

# Scattering of Sine-Gordon kinks on potential wells

Bernard Piette and W.J. Zakrzewski

*Department of Mathematical Sciences, University of Durham,  
Science Laboratories, South Road, Durham DH1 3LE, England*

(Dated: July 12, 2018)

We study the scattering properties of Sine Gordon kinks on obstructions in the form of finite size potential ‘wells’. We model this by making the coefficient of the  $\cos(\varphi) - 1$  term in the Lagrangian position dependent. We show that when the kinks find themselves in the well they radiate and then interact with this radiation. As a result of this energy loss the kinks become trapped for small velocities while at higher velocities they are transmitted with a loss of energy. However, the interaction with the radiation can produce ‘unexpected’ reflections by the well.

We present two simple models which capture the gross features of this behaviour. Both involve standing waves either at the edges of the well or in the well itself.

PACS numbers: 11.10.Lm,12.39.Dc,03.75.Lm

## I. INTRODUCTION

Recently [1] we have performed a detailed study of scattering properties of (2+1) dimensional topological solitons on potential wells. This work was based on the ‘baby’ Skyrme model, *ie* we used the Lagrangian density which consisted of three terms: the pure  $\mathcal{S}^2$  sigma model, the Skyrme and the potential terms:

$$\mathcal{L} = \partial_\mu \vec{\phi} \cdot \partial^\mu \vec{\phi} - \theta_S \left[ (\partial_\mu \vec{\phi} \cdot \partial^\mu \vec{\phi})^2 - (\partial_\mu \vec{\phi} \cdot \partial_\nu \vec{\phi})(\partial^\mu \vec{\phi} \cdot \partial^\nu \vec{\phi}) \right] - V(\vec{\phi}) \quad (1)$$

where

$$V(\phi) = \mu(1 - \phi_3^2). \quad (2)$$

The vector  $\vec{\phi}$  was restricted to lie on a unit sphere  $\mathcal{S}^2$  hence we put  $\vec{\phi} \cdot \vec{\phi} = 1$ .

To generate the potential well the coefficient of the potential term  $\mu$  was made  $x$  dependent. For  $x$  outside the well it had one value, say,  $\mu_{out}$  and inside the well, *ie* for  $a < x < b$  its value was reduced to  $\mu_{in}$ . This choice of  $\mu$  did not affect the vacuum (taken as  $\phi_3 = +1$ ); the skyrmion was given by a field configuration which varied from  $\phi_3 = +1$  far away from the position of the skyrmion to  $\phi_3 = -1$  at its position). Initially, the skyrmions were placed far away from the ‘well’ (so that all the variation of  $\phi_3$  from  $+1$  took place for  $x$  well away from the ‘well’, *ie* for  $x < a$ ).

The ‘skyrmions’ were then sent towards the well and their properties were studied. The obtained results have shown that when the solitons fall into the ‘well’ they get deformed and this deformation may excite the vibrational modes of the skyrmion and may lead to the skyrmions radiating away their excess of energy. In consequence, the skyrmions can get ‘trapped’ in the well or emerge from it with a reduced velocity. In [2] we presented a simple four mass model which apes the vibrational modes of the skyrmion and we showed that many of the observed scattering properties of skyrmions can be reproduced in this model - suggesting that their origin resides in the excitation of the lowest vibrational modes of the skyrmion.

Given this, it is important to check what happens in models in which solitons have fewer vibrational modes and so we have decided to look at the (1+1) dimensional Sine-Gordon model and see what happens when its kinks scatter on the potential wells.

In the next section we discuss our results obtained for the Sine-Gordon model. In this model we include a finite size, finite depth, potential well which is introduced by appropriately modifying the coefficient of the nonlinear term

in the Lagrangian. The results are qualitatively similar to what we have seen in the two-dimensional model and are not very different from the results obtained some time ago by Fei et al [3], in a work which involved the scattering of Sine-Gordon kinks on a one-point impurity.

Recently, Goodman and collaborators [4] have explained these old results [3] in a ‘two bounce’ resonance model. Their explanation is based on the interaction of the kink with the oscillation of the vacuum (around the impurity). Thus their model involves two degrees of freedom - the position of the kink  $x_0$  and the amplitude of the vacuum oscillation (at the impurity point)  $a$ . The model of Goodman et al has reproduced all the features of the results of the original simulations reported in [3]. Hence in the following section we introduce a similar model for our case which now involves a finite well of width  $2p$  and depth  $1 - \lambda$ . To do this we make an ansatz for an approximate field which describes the system. It involves a sine-Gordon kink which is allowed to alter its slope and we add to it two amplitudes of oscillation of the vacuum (at each end of the ‘well’). In section 3 we derive the Lagrangian for such an effective model from the original Lagrangian. As the model is somewhat crude we make some drastic approximations in our derivation of the Lagrangian but still find that the model reproduces the main features of the scattering reasonably well. Hence we believe the ideas of Goodman and collaborators to be correct and be more general in nature - thus showing that due to the interaction of the soliton with the radiation in the well its behaviour can be quite complicated and can result in the reflection of the soliton by the well; *ie* a process which is purely classical in nature but could be confused with a quantum behaviour. To confirm this further we introduce a further model (with a couple of radiation standing waves in the well) and again reproduce the main features of the full scattering process.

The last section presents some concluding remarks.

## II. SINE GORDON MODEL AND ITS KINKS.

We take the Lagrangian of the (1+1) dimensional Sine-Gordon model in the form

$$\mathcal{L} = \partial_\mu \varphi \cdot \partial^\mu \varphi - \lambda^2 \sin(\varphi)^2, \quad (3)$$

where, for the kink, the basic field  $\varphi$  goes from 0 at  $x = -\infty$  to  $\pi$  at  $x = \infty$ . In the static case its explicit form is

$$\varphi(x) = 2 \tan^{-1}(\exp(\theta(x - x_0))), \quad (4)$$

where  $x_0$  is the kink’s position and  $\theta$  is its slope. For (4) to be a solution of the equations of motion which follow from (3) we need to set  $\theta = \lambda$ .

To have a ‘well’ we set

$$\lambda = \begin{cases} 1 & \text{for } |x| > p \\ \lambda_0 & \text{for } |x| < p. \end{cases} \quad (5)$$

Clearly,  $\lambda_0 < 1$  describes a well while  $\lambda_0 > 1$  describes a barrier. As the two-dimensional studies gave more interesting results for the wells in this paper we restrict our attention to  $\lambda_0 < 1$ .

We have performed many numerical simulations, varying  $\lambda_0$  and  $p$  (the width of the well).

### A. Numerical Simulations

We have performed most of our simulations using a 10001 point lattice with the lattice spacing being 0.05. Hence our lattice extended from -50 to +50. The kink was initially placed at  $x_0 = -40$ . Its size was determined by  $\theta = 1$

which means that its field was essentially  $\varphi \sim 0$  for  $x < -45$  and  $\varphi \sim \pi$  for  $x > -35$ . Thus, there were no problems with any boundary effects (we have verified this by altering the lattice size and  $x_0$ ).

We have performed three sets of simulations; one involving a very narrow ‘well’ ( $p = 0.5$ ) and two involving a larger well ( $p = 5$ ) (one shallow -  $\lambda_0 = 0.8$  and one rather deep -  $\lambda_0 = 0.2$ ). In each case we sent the kink (originally at  $x_0 = -40$ ) towards the well varying its initial velocity. To do this we took the expression for a kink moving with velocity  $v$  *ie*

$$\varphi(x, t) = 2 \tan^{-1}(\exp(\gamma(x - x_0 - vt))), \quad \gamma = \frac{1}{\sqrt{1 - v^2}} \quad (6)$$

(obtained by Lorentz boosting (4) and setting  $\theta = 1$ ) and then used it to calculate the initial conditions ( $\varphi(x, 0)$  and  $\frac{\partial \varphi(x, 0)}{\partial t}$ ).

All our simulations were performed using a 4th order Runge-Kutta method for simulating the time evolution. The time step of our simulations was taken to be 0.0001. We used fixed boundary conditions and later we used also absorbing boundary conditions at the edges of the lattice. This was generated by successively decreasing the magnitude of  $\frac{\partial \varphi}{\partial t}$  for the last 50 points at both ends of the lattice.

### B. Deep Well

In the deep well case we took  $\lambda_0 = 0.2$  and  $p = 5$ . We have found that when the kink was in the well it radiated and so, when it finally emerged from the well its velocity was lower than the initial velocity. This was due to the fact that the well distorted the soliton which then began vibrating (*ie* its slope started oscillating). These vibrations were then gradually converted into radiation with the slope settling at its original value. The curve of the outgoing velocity as a function of the incoming one is shown in fig. 1. As is clear from the plot, the kink whose initial velocity is less than  $v_{cr} \sim 0.527$  gets trapped in the well. The curve is very smooth and, as expected, we note that for incoming velocities larger than  $v_{cr}$  the outgoing velocity is always larger than the incoming one demonstrating the loss of the kinetic energy of the kink through vibration resulting in radiation.

### C. Shallow Well

For a shallow well we took  $\lambda_0 = 0.8$  and still  $p = 5$ . This time the critical velocity is much smaller (as the well perturbs the kink much less). The curve of the outgoing velocity as a function of the incoming one is shown in fig. 2a.

Looking at the plot we note that there is some irregularity close to the threshold. Blowing it up (see fig. 2b)

we note that just below the critical velocity we also have some negative velocities (*ie* the whole process looks as if the kink was reflected by the well!). Thus in addition to trajectories like those in fig. 3a and fig. 3b we also have trajectories like those of fig. 3c

Of course - the reflected trajectory is somewhat unexpected; this is what one would expect in a quantum system but here we have a completely classical system and we have a reflection by the well. Clearly, this reflection must be somewhat related to the interaction of the deformed kink with the radiation that is present in the well. To look at this in more detail we have looked also at a very narrow well.

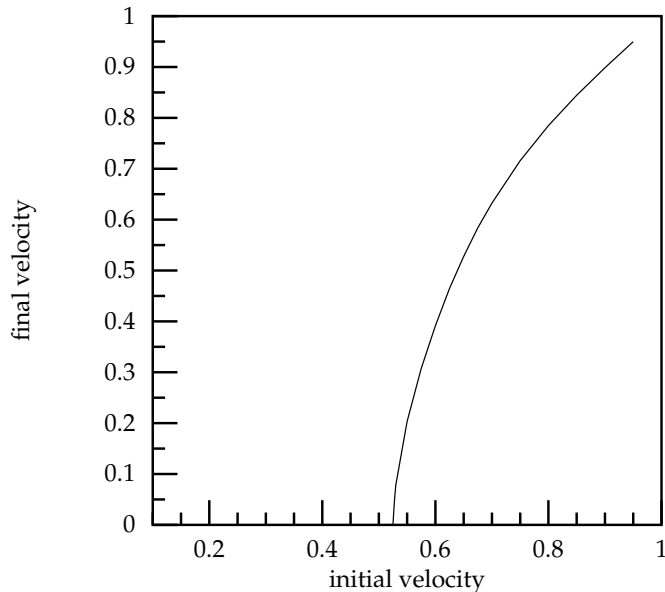


FIG. 1: Velocity of the kink leaving the well as a function of its velocity as it approaches the well.  $p = 5$ ,  $\lambda_0 = 0.2$ .

#### D. Very Narrow Well

This time we took  $p = 0.5$  and  $\lambda_0 = 0.2$ . The obtained curve of the velocities is shown in fig. 4a. Again we see an interesting behaviour close to the threshold - and blowing it up we get fig. 4b.

Are these results just numerical artifacts? To answer this question we have carried out several tests. First we changed the lattice size (increased the number of points, changed the lattice spacing) and changed the time step in the Runge Kutta scheme. However, the observed pattern of reflections was reproduced in all simulations. We have also varied the discretisation scheme and, among others, considered also the ‘topological discretisation’ of Speight and Ward [5]. All simulations using these discretisations exhibited similar patterns, with the values of the velocities essentially unchanged (the values changed in the fourth decimal points). Hence we believe the effect to be genuine and so we are left with having to explain its origin.

Performing a literature search we have found the above mentioned paper by Fei et al [3]. In that paper the authors studied the scattering of Sine-Gordon kinks on a one lattice point impurity (at one lattice site the potential  $\lambda\varphi^2$  was changed to a different value -  $\lambda'\varphi^2$ ). Fig. 11 of that paper looks amazingly similar to our fig. 4b. Of course, our potential corresponds to a superposition of defects of Fei et al so not surprisingly the pattern is more evident in a system involving a smaller well. However, the fact that the effect persists and is seen for larger wells suggests that

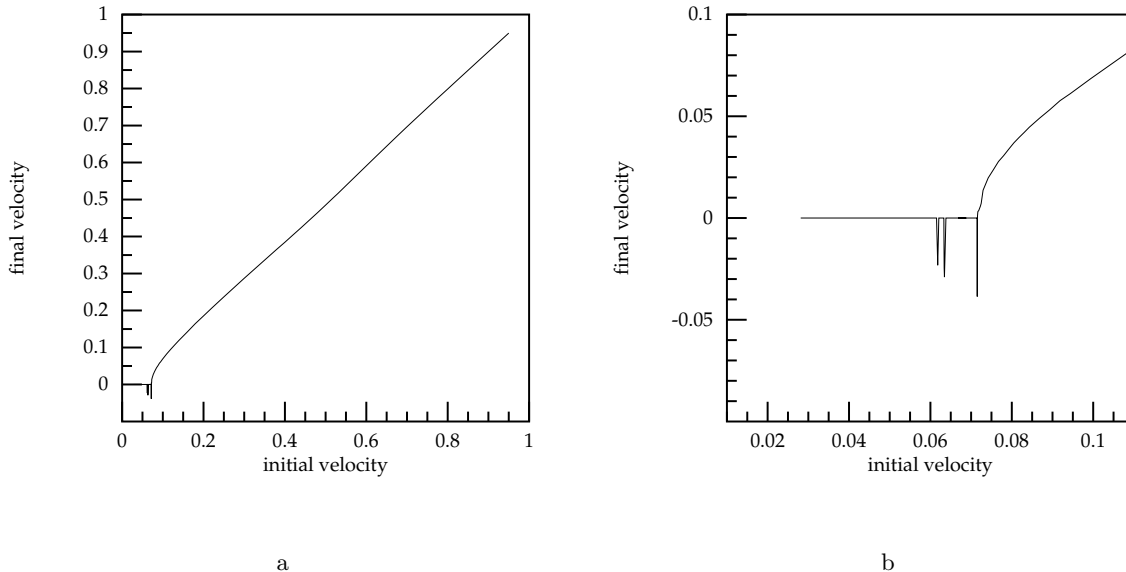


FIG. 2: Velocity of the kink leaving the well as a function of its velocity as it approaches the well ( $p = 5$ ,  $\lambda_0 = 0.8$ ). a) Full plot. b) A close up for small velocities.

the phenomenon is more fundamental in nature.

The phenomenon observed by Fei et al was recently explained by Goodwin et al [4] in terms of a two mode model involving the interaction of the kink with the radiation at the impurity point. Clearly in our case we have two special points (at the two 'edges' of the well where the potential changes). Hence it may make sense to develop a model based on oscillations at these two points. This is what we do in the next section.

### III. OUR EFFECTIVE MODEL

Following Goodman et al [4] we consider the following ansatz

$$\varphi(x, t) = 2 \tan^{-1} \exp(\theta(t)(x - x_0(t))) + a(t)g(x) + b(t)h(x), \quad (7)$$

where we take  $g(x)$  and  $h(x)$  in the form:

$$g(x) = \exp\left(-\frac{|x-p|}{2}D\right), \quad h(x) = \exp\left(-\frac{|x-p|}{2}F\right), \quad (8)$$

and

$$D = \begin{cases} A, & x > p \\ B, & x < p \end{cases}, \quad F = \begin{cases} B, & x > -p \\ A, & x < -p \end{cases}. \quad (9)$$

Thus we have allowed the kink to change its position  $x_0(t)$  and its slope  $\theta(t)$ , and  $a(t)$  and  $b(t)$  represent the excitations of the vacuum.

To obtain an effective model we put this expression for  $\varphi(x, t)$  into the Lagrangian density (3) and attempted to integrate it over  $x$ . However, as this leads to rather complicated expressions which we had not succeeded to calculate analytically we resorted to an expansion (in the perturbation due to the well). Hence we put  $\varphi = \varphi_0 + \delta\varphi$ , where

$$\varphi_0 = 2 \tan^{-1} \exp(\theta(t)(x - x_0(t))) \quad (10)$$

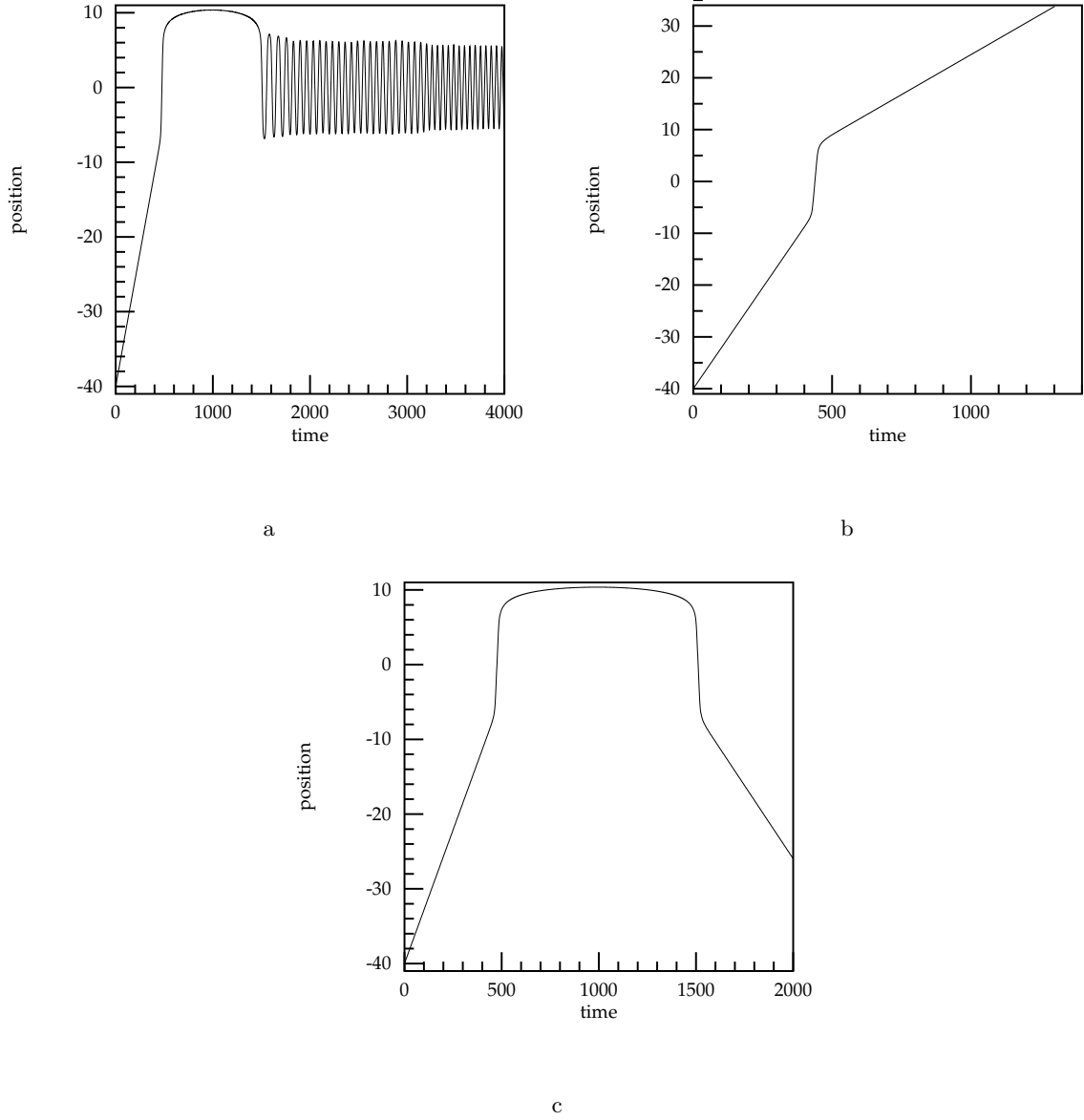


FIG. 3: Typical trajectories ( $p = 5$ ,  $\lambda = 0.8$ ). a) Below 'threshold' ( $v = 0.071535$ ), b) Transmitted ( $v = 0.077983$ ), c) Reflected ( $v = 0.071514$ ).

and

$$\delta\varphi = a(t)g(x) + b(t)h(x). \quad (11)$$

Next we expanded:

$$\sin^2(\varphi_0 + \delta\varphi) \sim \sin^2(\varphi_0) + \sin(2\varphi_0)\delta\varphi + \cos(2\varphi_0)(\delta\varphi)^2 \dots \quad (12)$$

Then as

$$\frac{\partial\varphi}{\partial t} = 2\cos^2\left(\frac{\varphi}{2}\right) \left[ \dot{\theta}(x-x_0) - \theta\dot{x}_0 \right] e^{\theta(x-x_0)} + \dot{a}g(x) + \dot{b}h(x) \quad (13)$$

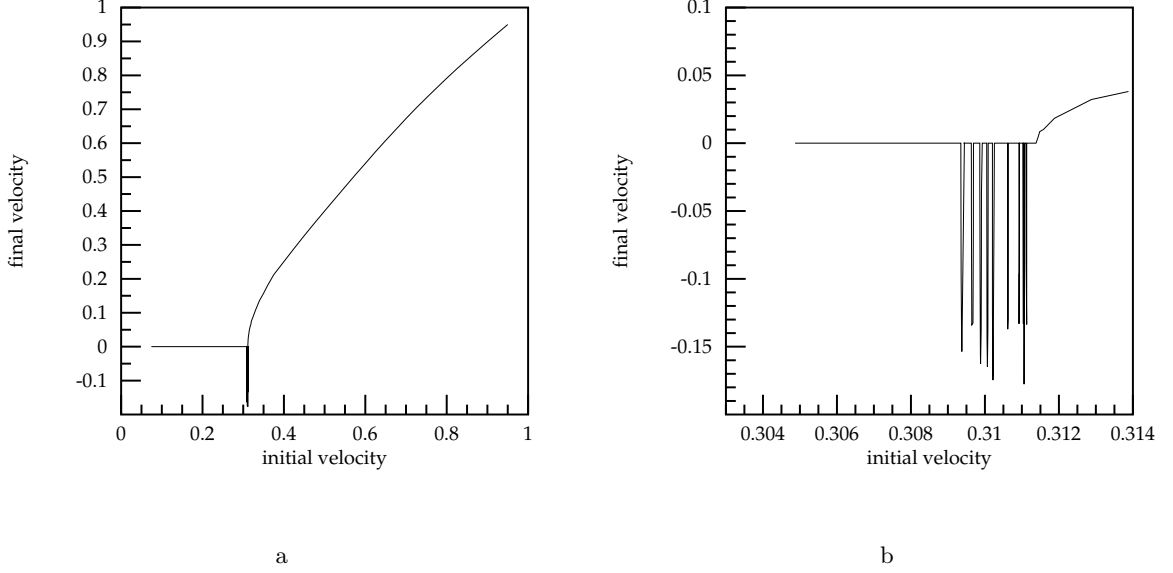


FIG. 4: Velocity of the kink leaving the well as a function of its velocity as it approaches the well ( $p = 0.5$ ,  $\lambda_0 = 0.2$ ). a) Full plot. b) A close up for small velocities.

we found that

$$T_1 = \int_{-\infty}^{\infty} dx \left( \frac{\partial \varphi_0}{\partial t} \right)^2 = \frac{1}{12} \frac{\pi^2 \dot{\theta}^2}{\theta^3} + \theta \dot{x}_0^2 \quad (14)$$

The  $\delta\varphi$  terms give us by themselves

$$T_2 = \frac{1}{2} (\dot{a}^2 + \dot{b}^2) \left( \frac{1}{B} + \frac{1}{A} \right) + \dot{a}\dot{b} \left[ \frac{4}{A+B} e^{-Bp} + \frac{2}{A-B} (e^{-pB} - e^{-pA}) \right]. \quad (15)$$

Finally, we calculated the ‘crossed terms’ and we got (for the terms involving  $\dot{x}_0$  and  $\dot{a}$  and  $\dot{b}$ )

$$T_3 = -2\theta \dot{x}_0 \dot{a} \frac{K}{1+K^2} \left[ \frac{1}{\theta + \frac{B}{2}} + \frac{1}{\frac{A}{2} - \theta} \right], \quad (16)$$

where  $K = \exp(\theta(p - x_0))$  and a similar expression for  $-2\theta \dot{x}_0 \dot{b}$ , except that this  $K$  was replaced by  $\tilde{K} = \exp(\theta(-p - x_0))$ . For the terms involving  $\dot{\theta}$  and  $\dot{a}$  we got

$$T_4 = 2\dot{\theta} \dot{a} \frac{K}{1+K^2} \left\{ \left[ \frac{1}{(\frac{A}{2} - \theta)^2} - \frac{1}{(\frac{B}{2} + \theta)^2} \right] + \frac{p(1-K^2)}{(1+K^2)} \left[ \frac{1}{\theta + \frac{B}{2}} + \frac{1}{\frac{A}{2} - \theta} \right] \right\} \quad (17)$$

The expression involving  $\dot{\theta} \dot{b}$  was again the same with  $K$  replaced by  $\tilde{K}$ . These expressions are not exact; we obtained them by making several approximations of the type

$$K \int_0^{\infty} dz \frac{e^{-(\theta + \frac{B}{2})z}}{1 + K^2 e^{-2\theta z}} \sim \frac{K}{1 + K^2} \frac{1}{(\theta + \frac{B}{2})}, \quad (18)$$

which should be reasonably reliable given the exponential form of the dependence of the integrands on  $z$  etc.

Next we calculated the contribution due to  $(\frac{\partial \varphi}{\partial x})^2$ . Performing the integrations, and making similar approximations as before we got

$$P_1 = \theta + \frac{(a^2 + b^2)}{8} + \frac{ab}{4} \left[ 4(A+B)e^{-Bp} + \frac{(A+B)^2}{2(A-B)} (e^{-pB} - e^{-pA}) \right] \quad (19)$$

plus terms linear in  $a$  and  $b$ . They are given by

$$P_2 = -\frac{A+B}{2} \left( \frac{1}{\frac{A}{2}-\theta} + \frac{1}{\frac{B}{2}+\theta} \right) \left( \theta a \frac{K}{1+K^2} + \theta b \frac{\tilde{K}}{1+\tilde{K}^2} \right). \quad (20)$$

Finally we had to add the  $\lambda^2 \sin^2(\varphi)$  terms. The contribution due to the well is given by

$$\begin{aligned} \lambda_0^2 \int_{-p}^p \sin^2(\varphi_0) dx &= \lambda_0^2 \int_{-p}^p \frac{e^{2\theta(x-x_0)}}{[1+e^{2\theta(x-x_0)}]^2} dx \\ &= \frac{\lambda_0^2}{\theta} \frac{\sinh(2\theta p)}{\cosh(2\theta x_0) + \cosh(2\theta p)}. \end{aligned} \quad (21)$$

The contribution due to  $\int_{-\infty}^{\infty} dx \lambda_0^2 \sin^2(\varphi)$  can be calculated in a similar way and we get

$$P_3 = \frac{\lambda_1^2}{\theta} \quad (22)$$

from the  $\varphi_0$  term,

$$P_4 = 2\lambda_1^2 \left( \frac{1}{\frac{A}{2}-\theta} + \frac{1}{\frac{B}{2}+\theta} \right) \left[ a \frac{K(1-K^2)}{(1+K^2)^2} + b \frac{\tilde{K}(1-\tilde{K}^2)}{(1+\tilde{K}^2)^2} \right] \quad (23)$$

from the terms linear in  $\delta\varphi$  and

$$P_5 = \frac{\lambda_1^2}{2} \left[ (a^2 + b^2) \left( \frac{1}{B} + \frac{1}{A} \right) + ab \left( \frac{4}{A+B} e^{-Bp} + \frac{2}{A-B} (e^{-pB} - e^{-pA}) \right) \right]. \quad (24)$$

Adding all these terms together we get the Lagrangian for our effective model. This Lagrangian is given by

$$\begin{aligned} L &= \frac{\pi^2 \dot{\theta}^2}{12 \theta^3} + \theta \dot{x}^2 + \frac{1}{2} (\dot{a}^2 + \dot{b}^2) B_0 + \dot{a} \dot{b} B_1 - 2\theta \dot{x}_0 (\dot{a} D_0(\theta) + \dot{b} D_1(\theta)) \\ &+ 2\dot{\theta} (\dot{a} D_2(\theta) + \dot{b} D_3(\theta)) - \theta - \frac{(a^2 + b^2)}{8} (A+B) - \frac{ab}{4} + \frac{A+B}{2} \theta (a D_0(\theta) + b D_1(\theta)) \\ &- 2\epsilon \lambda_1^2 D_6(\theta, x_0) - \frac{\lambda_1^2}{\theta} - 2\lambda_1^2 (a D_4(\theta) + b D_5(\theta)) - \lambda_1^2 \frac{ab}{2} B_1 - \lambda_1^2 \frac{(a^2 + b^2)}{2} B_0, \end{aligned} \quad (25)$$

where

$$B_0 = \frac{1}{B} + \frac{1}{A}, \quad B_1 = \frac{4}{A+B} e^{-pB} + \frac{2}{A-B} (e^{-pB} - e^{-pA})$$

and where the 7 functions  $D_i$   $i = 0, ..6$  are given by:

$$\begin{aligned} D_0(\theta) &= \frac{K}{1+K^2} \left[ \frac{1}{\theta + 0.5B} + \frac{1}{0.5A - \theta} \right], \\ D_2(\theta) &= \frac{K}{1+K^2} \left[ -\frac{1}{(\theta + 0.5B)^2} + \frac{1}{(0.5A - \theta)^2} \right] + p \frac{1-K^2}{1+K^2} \left[ \frac{1}{\theta + 0.5B} + \frac{1}{0.5A - \theta} \right], \\ D_4(\theta) &= D_0(\theta) \frac{1-K^2}{1+K^2}. \end{aligned}$$



The functions  $D_1(\theta)$  and  $D_5(\theta)$  have the same form as  $D_0(\theta)$  and  $D_4(\theta)$ , respectively, after the replacement  $K \rightarrow \tilde{K}$  and

$$D_3(\theta) = \frac{\tilde{K}}{1 + \tilde{K}^2} \left[ -\frac{1}{(\theta + 0.5B)^2} + \frac{1}{(0.5A - \theta)^2} \right] - p \frac{1 - \tilde{K}^2}{1 + \tilde{K}^2} \left[ \frac{1}{\theta + 0.5B} + \frac{1}{0.5A - \theta} \right].$$

Finally  $D_6(\theta, x_0)$  is given by

$$D_6(\theta, x_0) = \frac{1}{\theta} \frac{\sinh(2\theta p)}{\cosh(\theta(x_0 + p)) \cosh(\theta(p - x_0))}.$$

The derived Lagrangian involves 4 variables  $x_0, \theta, a$  and  $b$  but its equations are rather complicated. Hence we have solved them numerically. In the next section we discuss our solutions of the equations which follow from the Lagrangian (25).

#### IV. RESULTS IN OUR EFFECTIVE MODEL

We have looked at the equations for  $\theta$ ,  $x_0$  and  $a$  and  $b$ , which follow from the Lagrangian (25) and solved them numerically. As our initial conditions we took  $x_0 = -40$ ,  $\theta = 1$  and set, initially,  $a = b = 0$ . Of course, we also put  $\dot{a} = \dot{b} = \dot{\theta} = 0$  and studied the behaviour of our system as a function of  $\dot{x}_0$ . We also varied a little the parameters  $A$  and  $B$ , which appear in the description of the effects due to the well. For most of our work we used the values around 0.5 (and used the fact that we expect  $A^2 \sim \epsilon + B^2$ . To have the well similar to the one we used in the full simulation (shallow well) we put  $\epsilon \sim 0.16$ . This is due to the fact that the linearised equations (*ie* for the waves) differ, inside and outside the well, by a term proportional to  $(\lambda_0^2 - 1)u$ . In our case this translates to  $A^2 - B^2 \sim \epsilon$  and so for a shallow well we have  $\epsilon \sim 1 - \lambda_0^2 = 0.16$ . We simulated the time evolution using the 4th order Runge Kutta method and have found that the well distorts the kink quite strongly but, as expected, it can trap the kink like in the original Sine-Gordon model. However, as the effective system does not absorb energy after a few bounces the kink can escape (forwards or backwards). Of course in the real system there are many degrees of freedom of radiation which can get generated in the hole and such bounces are very rare. So to model these ‘extra’ modes of radiation which take the energy out of the modes we are describing we introduced an absorption of the oscillations of  $\theta(t)$ , *ie* we added a term proportional to  $\dot{\theta}$  in the equation for  $\theta$ . This has, indeed, reduced the oscillations in  $\theta$  and made the model more realistic.

In fig. 5 we present the curve of  $v_{out}$  as a function of  $v_{in}$  obtained in our model, *ie* based on the Lagrangian (25). We note that although our effective model is quite crude it reproduces fig. 3b rather well. Hence we believe that the mechanism of Goodman et al [4] explains the behaviour of the kinks in our case too. Of course, we could check this in more detail by making fewer approximations and, perhaps, performing the evaluation of all the difficult integrals numerically, but we are not sure that the extra effort required would be justified.

#### V. ANOTHER EFFECTIVE MODEL

Given that our effective model reproduces the results of our simulations rather well we have decided to check the generality of this observation - is this related to the existence of standing waves in the neighbourhood of the well or is our model somewhat unique. Hence we considered another model this time involving a standing wave in the well. The idea here is to explore further whether the reflections observed in the full model can be related to the interaction of the soliton with the waves in the well. Hence this time we have taken for our field configuration  $\varphi = \varphi_0 + \delta\varphi$ , where, as before,

$$\varphi_0 = 2 \tan^{-1} \exp(\theta(t)(x - x_0(t))) \quad (26)$$

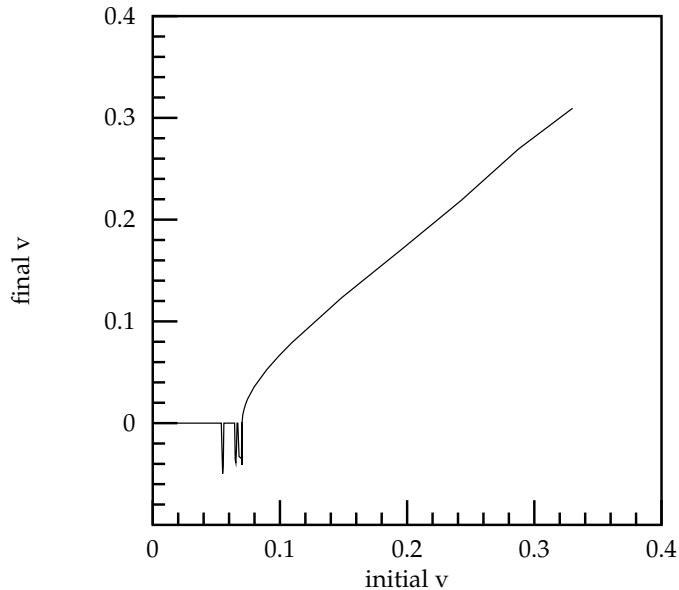


FIG. 5: Outgoing velocities as a function of incoming ones - in our effective model.

and

$$\delta\varphi = a(t)g(x). \quad (27)$$

This time for  $g(x)$  we have taken

$$g(x) = \cos\left(\frac{\pi x}{2p}\right) - \frac{1}{3}\cos\left(\frac{3\pi x}{2p}\right) \quad (28)$$

inside the well (*ie* for  $|x| < p$  and zero otherwise). Our  $g(x)$ , and its derivative, vanish at  $x = \pm p$  and the idea is that as the soliton enters the well its slope  $\theta(t)$  changes. This excites the modes described by  $g(x)$  and so  $a(t)$  becomes nonzero. This puts some energy into these modes which then interact with the soliton. Due to this interaction this energy can, every now and then, be given back to the soliton resulting in its reflection or transmission.

Like in the previous model, we have put the expression for  $\varphi$  into the original Lagrangian, integrated over  $x$  obtaining an effective model involving  $x_0$ ,  $\theta$  and  $a$ . Then we performed some simulations starting with a soliton originally far from the well moving with some velocity towards it. Like in the previous model we have absorbed energy through a term proportional to  $\frac{\partial\theta}{\partial t}$  in the equation for  $\theta$ . Also, like in the previous case we have found some reflections below the threshold for the scattering through the well. Their details depend a little on the strength of the absorption; at no absorption we have reflections, and transmissions forward, at much lower velocities, the higher absorptions kill

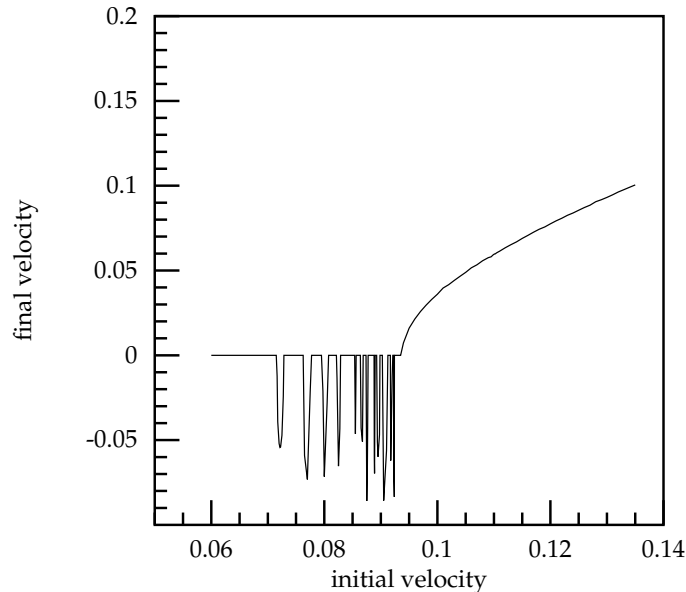


FIG. 6: Outgoing velocities as a function of incoming ones - in our second effective model.

the reflections and transmissions. They also raise the threshold for transmission. Of course, it is difficult to estimate reliably the degree of absorption as in the full model there are many modes of oscillations in the well. So in the end we have used very low absorption; then the threshold for transmission was close enough to what is seen in the full simulation but we had more reflections below threshold. To improve the model we should have used more modes in the well but this would have resulted in a more complicated model with more degrees of freedom. As we have only wanted to test our basic idea (that the reflections are due to the interaction of the soliton with radiation modes), in this paper, we decided to look at a model which is as simple as possible *ie* with a very few degrees of freedom. Our choice of two low lying modes was dictated by simplicity and the basic belief that the lower modes would get excited first and so are more important. In fig. 6 we present the curve of  $v_{out}$  as a function of  $v_{in}$  obtained in this (second) model (with a reasonable absorption). Once again, we see that the model reproduces well the pattern of the simulations of the full Sine-Gordon model (fig. 3b).

## VI. CONCLUSIONS

We have looked at a system involving a Sine-Gordon kink scattering on a ‘well’-like potential.

We have found that, like in (2+1) dimensions, when the kink was sent towards the well it gained some energy as it

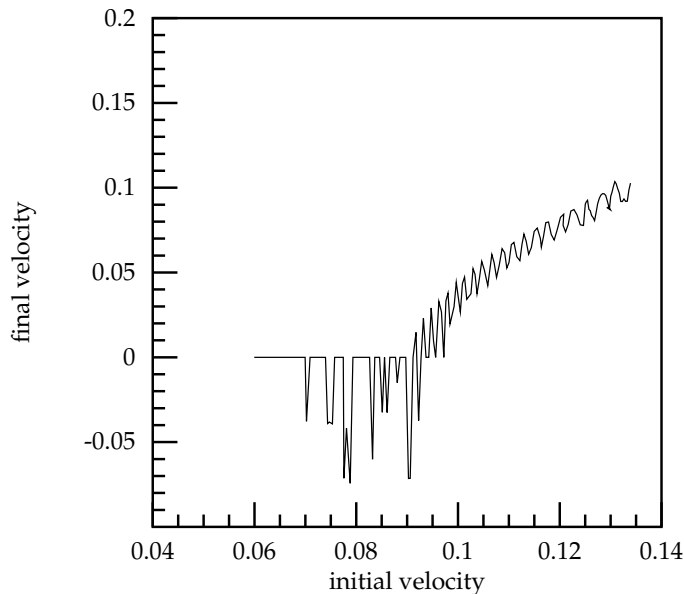


FIG. 7: Outgoing velocities as a function of incoming ones - in our second effective model without relativistic corrections.

entered the well. Some of this energy was converted into kinetic energy of the kink, some was radiated away. So when the kink tried to ‘get out’ of the well it had less kinetic energy than at its entry and, when this energy was too low it remained trapped in the well. However, as the soliton moved in the ‘well’ it interacted with the radiation in the well and at some specific values of the initial velocity this interaction resulted in the kink being ejected backwards from the well (with much reduced velocity). Thus, seen from outside, the well acted as if it reflected the kink, something which is seen in quantum systems but which is less well known in classical systems.

We have performed many numerical simulations to make sure that the observed behaviour is not an unexpected artifact of our numerical procedures and the pattern survived all applied tests. Hence we believe the effect to be genuine.

We have noted that a similar behaviour was observed many years ago by Fei et al who studied the scattering of kinks on a one-point impurity. This behaviour was recently explained by Goodman et al [4] as a two-bounce resonance between the kink and the oscillation of the defect. This has made us to consider two models of a similar nature. Both models are very simple, clearly too simple, but we wondered whether they would qualitatively reproduce the observed effects. Both involve kinks interacting with radiation and we generate this by taking an ansatz involving a kink (which can vary its position and slope) plus a couple of radiation modes. This ansatz is then put into the full equation which are then integrated out resulting in a model involving a few variables; namely, the position and the slope of the kink

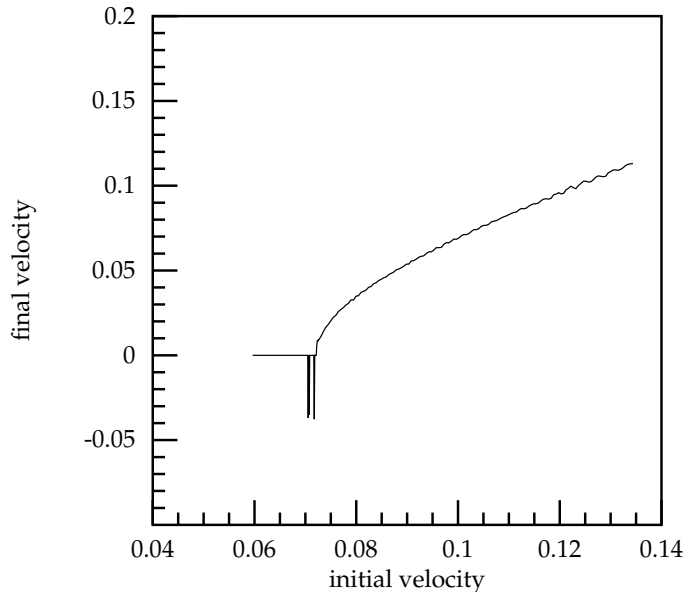


FIG. 8: Outgoing velocities as a function of incoming ones - in the full simulation without relativistic corrections

and the coefficients of the oscillation modes of the vacuum (modeling radiation).

The first model involved taking standing waves that are located at the edges of the well; the other one involved just one wave in the well. We have found that both models reproduced the main features of the observed behaviour quite well suggesting that the mechanism of Goodman et al is more general in nature and that, in general, the observed phenomenon of reflection of the solitons on the well is related to their interaction with the waves in the well. Of course, both models are too simplistic; to describe properly the full process we have to understand better which modes of radiation are important and why. This involves more work and is planned for the future. However, the work done so far suggests that we are on the right track and gives us encouragement for the further study. This is confirmed further by what we saw in a two-dimensional model [2] in which the solitons have genuine vibrational as well as radiation modes.

Incidentally, in our calculation we have used the correct initial condition *ie* with the correct relativistic factors ( $\gamma = \frac{1}{\sqrt{1-v^2}}$ ). Had we ignored them and used their nonrelativistic form (*ie* not modified  $\theta$  in (10) and (26)) we would have obtained instead of Fig. 6 the dependence which is shown in Fig. 7. We note an interesting oscillatory behaviour. Of course, this oscillation is overemphasised by the use of too few radiation modes but we wondered whether it would be seen in the full model too (*ie* whether the addition of further modes would wash them out). Hence we have redone the full simulations also without the relativistic factors. Our nonrelativistic curve is shown in fig. 8. We note the

extra oscillations. Their origin lies clearly in the fact that the absence of  $\gamma$  factors induces initial distortions resulting in the change of  $\theta$ . This affects the phase of the soliton and so alters its interaction with the wave in the well resulting in the curve shown in fig. 8. It is interesting to note that our effective models also reproduce these oscillations, thus giving further support for the validity of our claim that the interaction with the well proceeds through the generation of standing waves and their interference with the solitonic fields. Of course the agreement between the results of the full simulations and of the effective models is only qualitative in nature as in our effective models we used only some standing waves which were chosen somewhat ad hoc. To get a quantitative agreement we have to determine the relative importance of different waves - this problem is currently under consideration.

Several real physical systems are described by the sine Gordon equation, especially in solid state physics, and it would be interesting to see what the physical implications of a position dependant potential, like the one used in this paper, would be.

### Acknowledgements

This investigation is a natural follow up of the work on (2+1) dimensional topological solitons originally performed in collaboration with Joachim Brand. We would like to thank him for this collaboration.

- 
- [1] B.M.A.G. Piette, W.J. Zakrzewski and J. Brand, *J. Phys.* **A**, 1-10 (2005)
  - [2] B.M.A.G. Piette and W.J. Zakrzewski, preprint (2006)
  - [3] Z. Fei,, Yu.S. Kivshar, and L. Vazquez, *Phys. Rev.* **A 45**, 6019-6030 (1992)
  - [4] R.H. Goodman and R. Haberman, *Physica D* **195**, 303-323 (2004).
  - [5] J.M. Speight and R.S. Ward, *Nonlinearity* **7**, 475-484 (1994).